Stand-mediated DNA displacement for multiplexed analyte separation and detection

Christine Probst

A thesis submitted in partial fulfillment of the requirements for the degree of:

Master of Science

University of Washington

2012

Program Authorized to Offer Degree:
Department of Bioengineering
University of Washington

Abstract

Stand-mediated DNA displacement for multiplexed analyte separation and detection

Christine Probst

Chair of the Supervisory Committee:

Xiaohu Gao, Ph.D.

Department of Bioengineering

Medical and biological research is progressing at an astonishing rate, with an increasing emphasis on the understanding of complex biological systems. At the heart of this revolution has been the development of modern researching technologies, especially those that take more biological measurements, with increasing sensitivity and precision, at higher speed and lower cost. For example, immunomagnetic separation has become an essential tool for high throughout and low cost isolation of biomolecules and cells from heterogeneous samples. However, as magnetic selection is essentially a “black-and-white” assay, its application has been largely restricted to single-target and single-parameter studies. This document describes the development of an immunomagnetic separation technology that can quickly sort multiple targets at high yield and purity using selectively displaceable DNA linkers. Overall, this work provides strong evidence for the benefits of this approach for experiments requiring multiplexed immunomagnetic separation, can be readily adopted for specific applications requiring high throughput selection of multiple targets, and further adapted for selection of a single target based on multiple surface epitopes.

Contents

List of Figures

List of Tables

Introduction

Magnetic separation technologies have played a critical role in a variety of biomedical applications ranging from molecular diagnostics to cell-based therapy [1-4]. In contrast to other separation technologies, such as spatial separation via microarrays [5] or optical separation using fluorescence-activated cell sorting [6, 7], magnetic separation offers major advantages in terms of throughput and cost [8, 9]. However, as selection is based on a single parameter (magnetization), only one target can be isolated at a time. Thus, intricate protocols are necessary to separate multiple targets from a sample (multi-target), or to isolate a single target based on multiple surface epitopes (multi-parameter) [10]. Given that emerging research demands interrogation of increasingly complex and heterogeneous systems, in particular within the fields of immunology and oncology, there is a clear need for innovative magnetic separation technologies that enable multiplexed target sorting with high throughput, purity, and yield.

Several strategies have been proposed to incorporate multiplexing potential into magnetic separation. One promising approach is to use the size tunable properties of magnetic nanoparticles for simultaneous isolation of several targets [11-15]. For example, Adams et al. [16] described a multi-target MACS, which applied microfluidics and high-gradient magnetic fields to separate 2 bacterial targets using 2 distinct magnetic tags at >90% purity and >500 fold enrichment. However, multi-target sorting through ‘physical’ encoding of magnetic particles requires sophisticated instrumentation to spatially resolve each tag, and remains highly limited by the number of discrete magnetic tags that can be reliably separated. In a more straightforward approach, multiplexed separation can be achieved through multiple sequential rounds of single-target magnetic selection (Figure 1a). As an example, Semple et al. [17] used this method to sort CD4+ and CD19+ lymphocytes in a 4-hour procedure. Yet, despite its simplicity, not only is sequential sorting time-consuming, lengthy separation protocols often result in an

alteration of the biological state of the target (e.g. gene expression and/or viability of cells) [18], rendering such an approach unsuitable for many applications.

Complementary to the challenge of spatial or temporal segregation of target-carrying magnetic particles is the issue of incorporating multiplexing capability within the target capture method itself. Magnetic selection can be applied in one of two formats: (1) direct selection, where the affinity ligand is directly coupled to the magnetic nanoparticle, and (2) indirect selection, where targets are first incubated with an excess of primary affinity ligand and then captured by magnetic particles via secondary affinity ligand. As the indirect method allows for optimal affinity ligand orientation on target, a 'signal amplification' effect is observed, improving yield and purity [9]. Furthermore, the indirect method enables utilization of a wide range of commercial affinity ligands without the need for further modification. At the same time, this approach is particularly challenging to multiplex, given the limitations in selectivity of primary-secondary affinity ligands (e.g. biotin-streptavidin and primary-secondary antibody links). In this regard, DNA-antibody conjugates represent a powerful tool for multiplexed indirect selection, first demonstrated by Heath et al. [5] on DNA microarray platform. However, the small surface area of microarray chips hampers large-scale sorting applications. In this context, incorporation of molecular encoding *into* the conventionally single-parameter magnetic selection platform holds the key to achieving truly multiplexed, high-throughput target sorting.

This report describes a rapid multi-target immunomagnetic sorting technology that combines extensive multiplexing capacity of DNA-antibody conjugates and high selectivity, throughput, and simplicity of magnetic isolation by employing a unique sorting approach through strand-mediated displacement (SMD) of DNA linkers. A key insight for this work was that multiplexing selection through specific DNA sequences could offer simultaneous selection of multiple target populations from a heterogeneous sample, followed by quick isolation of

individual targets through SMD, inspired by the fast kinetics and selectivity of SMD in DNA motors and DNA walkers [19-22]. The major steps of SMD for multi-target sorting are illustrated in Figure 1b. In the first step, antibodies encoded with distinct DNA sequences (encoding probe, EP) bind their identifying antigen on target populations. Next, magnetic beads (MBs) coated with capture probes (CPs), which partially hybridize with their corresponding EPs, enable simultaneous magnetic selection of all targets of interest. In the second step, the magnetically enriched targets are released one population at a time through SMD upon addition of a displacement probe (DP). Probe assembly is schematically illustrated in Figure 1c. The DP binds selectively to an exposed 'toehold' region on the CP, and then 'unzips' the EP from its original binding site due to the longer complementarity between CP and DP, thus breaking the MB-target link. In this way, multiple targets can be quickly isolated through a serial addition of DPs. In direct contrast to the conventional multi-cycle magnetic separation (Figure 1a), SMD technology employs only a single round of slow immunorecognition, and the following SMDs are a remarkably rapid process (with a sub-second displacement half-time) [23]. Therefore, with sorting of N targets (N>1), our technology should offer significantly shortened assay time (N x Y hours *vs.* Y hours + rapid SMDs for assay time of Y hours), which is highly desired for preserving the native state and bio-functionality of isolated targets.

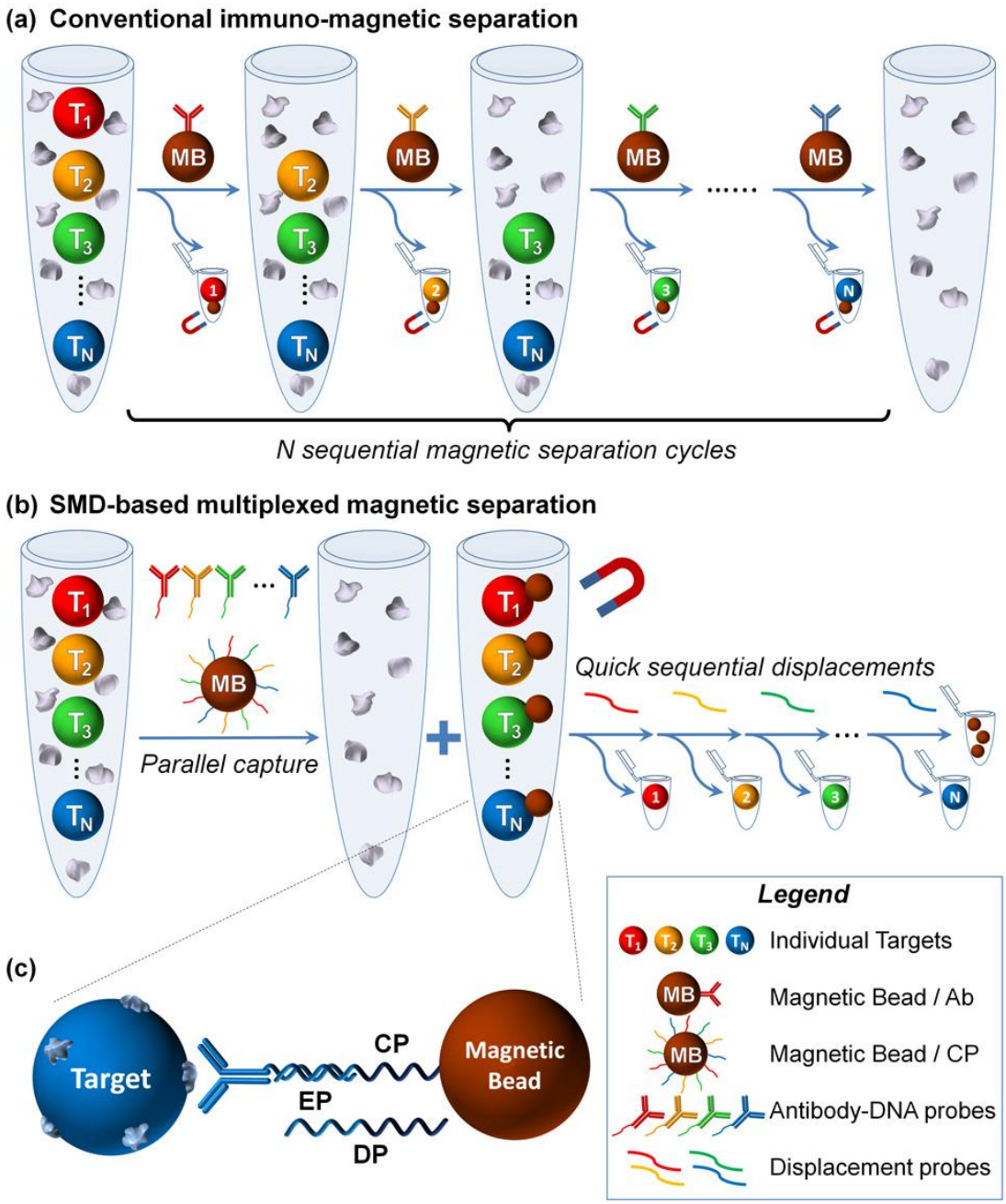

Figure 1. Schematic of multi-target immunomagnetic sorting. (a) Conventional sorting of multiple targets involves lengthy sequential magnetic isolation steps. (b) In contrast, SMD-based sorting technology captures all targets of interest simultaneously, followed by a rapid sorting through release of MB-Target link. (c) Target is captured through immunorecognition by DNA-encoded antibody and partial hybridization with CP on MB. Selective target release is

achieved through sequence-specific EP displacement due to a more favorable hybridization between CP and DP.

Abbreviations

MACS, magnetic-activated sorting; DNA, deoxyribonucleic acid; Ab, antibody; IgG, immunoglobulin G; SMD, strand-mediated displacement; CP, capture probe; EP, encoding probe; DP, displacement probe; MB, magnetic bead.

Materials

Fluorescent beads (Bangs Laboratories) 5-6 µm in diameter doped with 4 different organic dyes (Glacial Blue 360/450nm excitation/emission maxima, Dragon Green 480/520nm, Suncoast Yellow 540/600nm, and Flash Red 660/690nm) were used as a model system for development and characterization of the SMD technology. Each bead features surface carboxylic acid functional groups (with parking area between 37 and 174 $Å^2$/surface group) suitable for covalent conjugation with biomolecules. Magnetic beads (Dynabeads MyOne Streptavidin C1, Invitrogen) are 1 µm in diameter and feature streptavidin coating for easy assembly with biotinylated DNA probes. Purified IgG from human, mouse, and rabbit serum as well as whole goat anti-human, anti-mouse, and anti-rabbit IgG were purchased from Sigma-Aldrich. All antibodies were obtained in 1x PBS without carrier proteins or stabilizing reagents. Biotinylated goat anti-human, anti-mouse, and anti-rabbit IgG were either purchased from Sigma-Aldrich or prepared in house using EZ-Link NHS-PEG4-Biotin (Thermo Scientific). DNA probes were purchased from Integrated DNA Technologies. Sequences were optimized to minimize secondary structures and homology with mismatched DNA sequences at room temperature. Encoding probes (EPs) were synthesized with primary amine functional group at the 5' end for covalent conjugation with antibodies. Capture probes (CPs) were synthesized with a biotin tag at the 5' end for assembly with streptavidin-coated MBs. Both CPs and EPs included a 5’ 10A spacer to allow for flexibility at the bead interface. All DNA

probes were purified with HPLC, reconstituted in DNAase-free water (Thermo Scientific) at 100 µM, and stored at -20^{0}C. Sequences of DNA probes are summarized in Table 1.

Methods

Preparation of DNA-antibody conjugates

Functionalization of antibodies with encoding DNA sequences was achieved by covalent conjugation between primary amine groups present on antibody and the 5'-end primary amine group on DNA. First, IgG was activated with S-HyNic (succinimidyl-6-hydrazino-nicotinamide, Solulink) heterobifunctional cross-linker, which introduces aromatic hydrazine group: 100 µL 1 mg/mL IgG in 100 mM PBS was mixed with 2 µL 10 mM S-HyNic (in DMF) and incubated for 2 hours. At the same time, EP was activated with S-4FB (N-succinimidyl-4-formylbenzamide, Solulink) heterobifunctional cross-linker, which converts primary amine into aromatic aldehyde group: 100 µL 50 µM EP in 100 mM PBS was mixed with 2.5 µL 100 mM S-4FB (in DMF) and incubated for 2 hours. Excess cross-linkers was then removed by passing both activated IgG and EP through Zeba spin desalting columns (Thermo Scientific), and buffer was exchanged to 100 mM MES, pH5. Finally, activated IgG and EP were conjugated through formation of bis-arylhydrazone bond between aromatic hydrazine and aromatic aldehyde groups: IgG and EP were mixed together at ~20x molar excess of EP, reacted for 4 hours, and buffer-exchanged into 10 mM PBS with Zeba spin desalting columns. All reactions were performed at room temperature. DNA-antibody conjugates were stored at 4^{0}C and used within 2 months after preparation.

Preparation of antigen-coated fluorescent beads

IgGs purified from human, rabbit, and mouse serum were covalently linked to the surface of red, green, and blue fluorescent beads, respectively. Covalent conjugation was achieved via 2-step carbodiimide-mediated cross-linking between primary amines on IgG and carboxylic acid groups on bead surface. First, fluorescent beads were washed and suspended in MES buffer (pH 4.7) with 0.01% Tween-20 at 0.1 w/v% (~10^7 beads/mL) and activated for 15 minutes upon addition of 10 mg/mL 1-Ethyl-3-(3-dimethylaminopropyl)carbodiimide (EDC, Sigma-Aldrich) and 10 mg/mL *N*-hydroxysulfosuccinimide (sulfo-NHS, Thermo Scientific). Activated beads were washed by centrifugation (at 3000 g for 2 minutes) twice using 50mM Borate buffer (pH 8.4) with 0.01% Tween-20 to remove excess reactants and then incubated with IgG at 2.5 mg/mL in Borate buffer with 0.01% Tween-20 for 4-8 hours for covalent cross-linking. IgG-conjugated microspheres were washed 4 times to remove excess IgG, resuspended in 10mM PBS with 0.5% Bovine Serum Albumin (BSA, Sigma-Aldrich), and stored at 4^0C.

Validation of antigen coating on the surface of fluorescent beads

Presence of target-specific surface antigen (mouse, rabbit, or human IgG) on the surface of each fluorescent bead population was tested via labeling with biotinylated goat anti-mouse, anti-rabbit, or anti-human IgG followed by staining with quantum dot probes functionalized with streptavidin (Qdot 655 streptavidin conjugate, Invitrogen). PBS with 0.5% BSA was used as incubation and washing buffer throughout the experiment. All incubation steps were carried out at room temperature under gentle rotation. All washing steps were done through

centrifugation at 3000 g for 2 minutes. Each bead type was resuspended in 400µL buffer at a final concentration of $1x10^6$ beads/mL and split into 4 test volumes 100µL each. To 3 of the 4 samples, biotinylated IgGs were added at 0.2 µg/mL, incubated for 30 minutes, washed 3 times, and resuspended with 100µL buffer. The forth sample (control) was incubated with only 0.5% BSA/PBS and washed in the same fashion. Then QDot655-streptavidin probes were added to each sample at 1nM final concentration, incubated for 30 minutes, washed with buffer 4 times, and finally washed with water once. Pellets were resuspended in 10µL water, spotted onto glass cover slips, allowed to dry, and imaged at high magnification. Wide UV filter cube was used for imaging of all fluorescent beads and quantum dots (as UV light provides sufficient excitation energy for all fluorophores). Hyper-spectral imaging and further image analysis with Nuance software enabled unmixing of fluorescence signal components and direct quantitative analysis of Qdot staining intensity on the surface of fluorescent beads. False-color composite images were obtained by merging individual channels.

Study of target capture and release kinetics

Green fluorescent beads conjugated with rabbit IgG were used for the study of target capture and release kinetics. PBS with 0.5% BSA was used throughout all steps of this study. All incubation steps were performed under gentle rotation at room temperature unless noted otherwise. The conditions for capture experiments are outlined in Table S2. In step 1a, target beads were incubated with capture antibodies (with conjugated biotin or EP) for immunorecognition: 10^6 fluorescent beads/mL were mixed with capture antibodies at final antibody concentration of 2.5 µg/mL in 100 µL buffer and incubated for 30 minutes. Meanwhile, in step 1b, biotinylated CPs were immobilized onto streptavidin-coated magnetic beads: 10^7

MBs were mixed with CPs at final DNA concentration of 1 μM and incubated for 30 minutes. Fluorescent beads were washed through centrifugation (at 3000 g for 2 minutes) 4 times to remove excess antibody, while MBs were washed 4 times with a magnet to remove excess CPs. Fluorescent beads were then mixed with the magnetic fraction at a ratio of 50 MBs per fluorescent bead. For study of capture kinetics, the mixture was washed 3 times on the magnet following 5, 15, 30, and 60 minute incubation periods; supernatant fractions were pooled, and the MB-bound fraction was resuspended in equal volume. For study of target release kinetics, MB-bound fluorescent beads were prepared using the protocol described above (Condition 2 in Table 2). The conditions for SMD experiments are outlined in Table 3. Displacement probe (DP) was added to the mixture at 5 μM final concentration, and the solution was gently mixed for ~30 seconds with pipette. MB-bound fraction was separated with a magnet after 1 minute and 60 minute incubation periods. For both capture and release studies, reproducibility was evaluated by conducting three independent trials. For fluorescence measurement samples were placed into a 96-well black flat-bottom plate (Corning). Fluorescence in MB-bound and supernatant fractions was measured with fluorescence plate reader (Infinite M200, Tecan) at 480/541 nm excitation/emission wavelengths and constant gain. Measurements were averaged over 4 quadrants of each well to correct for inhomogeneous sedimentation of fluorescent beads. Equal volume of PBS with 0.5% BSA was used as a baseline, which was subtracted from all fluorescence readings. Fraction captured was calculated as the baseline-corrected fluorescence in MB-bound fraction divided by the sum of the baseline-corrected fluorescence in MB-bound fraction and supernatant.

Study of target capture specificity (from a 4-bead mix)

Three sets of "target" fluorescent beads were prepared: green beads were coated with rabbit IgG, blue beads with mouse IgG, and red beads with human IgG. Uncoated yellow beads were used as an "impurity" fraction. PBS with 0.5% BSA was used as incubation and washing buffer throughout this study. All incubation steps were performed under gentle rotation at room temperature. Purity of isolated fractions was quantitatively measured with flow cytometry (method described separately) and qualitatively evaluated with fluorescence microscopy (method described separately). Three independent trials for each experiment were conducted to evaluate reproducibility.

Part A (Specificity of antibody-antigen recognition for biotinylated IgGs): Four bead populations were pooled in even proportions into a single centrifuge tube to a total final concentration of $4x10^6$ beads/mL and split into 4 test volumes 100µL each. To 3 of the 4 samples, biotinylated Abs against rabbit, mouse, or human IgG were added at 0.2 µg/mL, incubated for 15 minutes, washed through centrifugation (at 3000 g for 2 minutes) 4 times to remove excess Abs, and resuspended with 100µL buffer. The forth sample (control) was incubated with buffer only and washed in the same fashion. Next, fluorescent beads were mixed with streptavidin-coated MBs at a ratio of 50 MBs per target fluorescent bead and incubated for 30 minutes. Each sample was then separated on a magnet for enrichment and isolation of green, blue, or red beads from the initial 4-color mixture. The magnetic fraction was washed 3 times, the supernatant fractions were pooled together, volumes of magnetic and supernatant fractions were equalized, and the absolute number of fluorescent beads in each fraction was counted with flow cytometry. All conditions tested are summarized in Table 4.

Part B (Specificity of antibody-antigen recognition for DNA-antibody conjugates): Four bead populations were pooled in even proportions into a single centrifuge tube to a total final concentration of $4x10^6$ beads/mL and split into 4

test volumes 100µL each. To 3 of the 4 samples, DNA-antibody conjugates against rabbit, mouse, or human IgG were added at 2 µg/mL, incubated for 15 minutes, washed through centrifugation (at 3000 g for 2 minutes) 4 times, and resuspended with 100µL buffer. The fourth sample (control) was incubated with buffer only and washed in the same fashion. Meanwhile, MBs with CPs (CP1, CP2, or CP3) were prepared by mixing 10^7 MBs with CPs at final DNA concentration of 1 µM, incubating for 15 minutes, and washing 4 times with a magnet. The fluorescent beads were then mixed with CP-MBs complementary to the capture DNA-antibody conjugate at a ratio of 50 MBs per target fluorescent bead and incubated for 30 minutes. Each sample was then separated on a magnet for enrichment and isolation of green, blue, or red beads from the initial 4-color mixture. The magnetic fraction was washed 3 times, the supernatant fractions were pooled together, volumes of magnetic and supernatant fractions were equalized, and the absolute number of fluorescent beads in each fraction was counted with flow cytometry. All conditions tested are summarized in Table 5.

Part C (Specificity of complementary DNA hybridization for EP-CP oligonucleotide pairs): Each "target" fluorescent bead type was separately labeled with its corresponding DNA-antibody conjugate. Fluorescent beads at a final concentration of $1x10^6$ beads/mL in a 100µL test volume were mixed with 2 µg/mL IgG-DNA, incubated for 15 minutes, and washed through centrifugation (at 3000 g for 2 minutes) 4 times. Then the three "target" bead populations and "impurity" yellow beads were mixed together at even proportions to a total final concentration of $4x10^6$ beads/mL. This way, potential nonspecific antigen-antibody binding was circumvented, and specificity of oligonucleotide hybridization could be independently assessed. Meanwhile, MBs with CPs (CP1, CP2, or CP3) were prepared by mixing 10^7 MBs with CPs at final DNA concentration of 1 µM and incubating for 15 minutes, and washing 4 times with a magnet. Magnetic beads with no CP were used as a control. The fluorescent beads were then mixed with CP-MBs corresponding to capture of a single target by

DNA hybridization at a ratio of 50 MBs per target fluorescent bead and incubated for 30 minutes. Each sample was then separated on a magnet for enrichment and isolation of green, blue, or red beads from the initial 4-color mixture. The magnetic fraction was washed 3 times, the supernatant fractions were pooled together, volumes of magnetic and supernatant fractions were equalized, and the absolute number of fluorescent beads in each fraction was counted with flow cytometry. All conditions tested are summarized in Table 6.

Study of strand-mediated displacement specificity for target release (from a 4-bead mix)

Three sets of "target" fluorescent beads were prepared for this experiment: green beads were coated with rabbit IgG, blue beads with mouse IgG, and red beads with human IgG. Uncoated yellow beads were used as an "impurity" fraction. PBS with 0.5% BSA was used as incubation and washing buffer throughout this study. All incubation steps were performed under gentle rotation at room temperature. Separately, each "target" bead type was labeled with its corresponding DNA-antibody conjugate. Fluorescent beads at a final concentration of $1x10^6$ beads/mL in a 100µL test volume were incubated with 2 µg/mL DNA-antibody conjugate for 15 minutes, and washed through centrifugation (at 3000 g for 2 minutes) 4 times. Then the three "target" bead populations and "impurity" yellow beads were mixed together at even proportions to a total final concentration of $4x10^6$ beads/mL. This way, weak nonspecific antigen-antibody binding/unbinding was circumvented, and specificity of target release via SMD could be independently assessed. Meanwhile, MBs with CPs (CP1, CP2, and CP3) were prepared by mixing $3x10^7$ MBs with CPs at total final DNA concentration of 3 µM, incubating for 15 minutes, and washing on a magnet 4 times. For capture of all 3 targets, fluorescent beads were mixed with CP-MBs

at a ratio of 50 MBs per target fluorescent bead and incubated for 30 minutes. Each sample was then separated on a magnet for enrichment and isolation of green, blue, or red beads from the initial 4-color mixture. The magnetic fraction was washed 3 times. Following magnetic capture, displacement probe corresponding to release of a single target (DP1: green, DP2: blue, DP3: red) was added to the sample at 5 µM final concentration, mixed gently with pipette for 1 minute, and then placed immediately on the magnet for collection of released beads in the supernatant. The sample was washed 3 times, and the supernatant fractions were pooled together. Purity of isolated fractions was quantitatively measured with flow cytometry (method described separately) and qualitatively evaluated with fluorescence microscopy (method described separately). Three independent trials were conducted to evaluate reproducibility. All conditions tested are summarized in Table 7.

4-color bead sorting with SMD technology

Three sets of "target" fluorescent beads were prepared for this experiment: green beads were coated with rabbit IgG, blue beads with mouse IgG, and red beads with human IgG. Uncoated yellow beads were used as an "impurity" fraction. The four populations were pooled in even proportions into a single centrifuge tube to a total final concentration of $4x10^6$ beads/mL. DNA-antibody conjugates (Ab-EP) against rabbit, mouse, and human IgG were added to the mixture at a final concentration of 2.5 µg/mL each and incubated for 30 minutes. Meanwhile, 3 different CPs (CP1, CP2, and CP3) were mixed at a 1:2:2 ratio (5 µM total) and incubated with $3x10^7$ MBs for 30 minutes. Fluorescent beads were washed through centrifugation (at 3000 g for 2 minutes) 4 times to remove excess antibody, and MBs were washed 4 times with a magnet to remove excess CPs. The fluorescent beads were then mixed with MB-CP at a ratio of 50 MBs per

target fluorescent bead and incubated for 30 minutes. The sample was then separated on a magnet for enrichment and isolation of green, blue, and red beads from yellow bead "impurity". The sample was washed 3 times, and the supernatant fractions were pooled together. Following magnetic capture, DP3 (corresponding to red beads) was added to the sample at 5 µM final concentration, mixed gently with pipette for 1 minute, and then placed immediately on the magnet for collection of released beads in the supernatant. The sample was washed 3 times, and the supernatant fractions were pooled together. In the same way, displacement probes corresponding to blue and green beads (DP2 and DP1 respectively) were added sequentially, mixtures were washed 3 times, and supernatants were pooled. The remaining MB-bound fraction was also resuspended in equal volume of buffer to evaluate the amount of beads that were not released. PBS with 0.5% BSA was used throughout all steps of this study. All incubation steps were performed under gentle rotation at room temperature unless noted otherwise. Purity of isolated fractions was quantitatively measured with flow cytometry (method described separately) and qualitatively evaluated with fluorescence microscopy (method described separately). Three independent trials were conducted to evaluate reproducibility.

4-color bead sorting with sequential streptavidin-mediated target capture

Three sets of "target" fluorescent beads were prepared for this experiment: green beads were coated with rabbit IgG, blue beads with mouse IgG, and red beads with human IgG. Uncoated yellow beads were used as an "impurity" fraction. The four populations were pooled in even proportions into a single centrifuge tube to a total final concentration of $4x10^6$ beads/mL. First, for red bead capture, biotinylated goat anti-human antibody was added to the sample at 0.2 µg/mL,

incubated for 15 minutes, and washed 4 times with centrifugation (at 3000 g for 2 minutes). The sample was then incubated with streptavidin-coated MBs (at 50 MBs per target bead ratio) for 30 minutes. The magnetic fraction was collected with the magnet to isolate captured "target" beads and washed 3 times. The supernatants with unbound beads were pooled together, pelleted through centrifugation (at 3000 g for 2 minutes), and resuspended back to the original sample volume of 100 µL for subsequent magnetic capture steps. In the same way, capture of blue and green "target" beads was performed through serial incubation with biotinylated secondary antibody (goat anti-mouse and goat anti-rabbit respectively), washing, incubation with MB-streptavidin, and magnetic collection. PBS with 0.5% BSA was used throughout all steps of this study. All incubation steps were performed under gentle rotation at room temperature. Purity of isolated fractions was quantitatively measured with flow cytometry (method described separately) and qualitatively evaluated with fluorescence microscopy (method described separately). Three independent trials were conducted to evaluate reproducibility.

Study of SMD-based sorting selectivity at varying target abundance

Two sets of "target" fluorescent beads were prepared for this experiment: red beads were coated with human IgG, blue beads with mouse IgG. Samples were prepared at a blue: red bead ratio at 1:1, 1:5, 1:20, and 1:100 by maintaining the concentration of red bead at $1x10^6$ beads/mL and reducing amount of blue beads accordingly. To evaluate the performance of SMD technology during target capture at decreasing target concentrations, sample purity achieved with capture via biotin-streptavidin bond formation was compared to sample purity achieved with capture via oligonucleotide hybridization. For each blue: red bead ratio, the

fluorescent beads were incubated with either biotinylated antibodies (goat anti-mouse, 0.2 µg/mL) or DNA-antibody conjugates (goat anti-mouse conjugated to EP2, 2.0 µg/mL) for 15 minutes and washed 4 times with centrifugation (at 3000 g for 2 minutes). Meanwhile, CP2-coated MBs were prepared by mixing $1x10^7$ MBs with CP2 at final DNA concentration of 1 µM, incubating for 15 minutes, and washing 4 times with magnet to remove excess CPs. Next, MB-Streptavidin (for samples previously incubated with biotinylated antibodies) or MB-CP2 (for samples previously incubated with DNA-antibody conjugates) were added to the sample at a constant concentration of 50 MBs per red fluorescent bead, incubated for 30 minutes, and isolated with using the magnet. Each magnetic fraction was washed 3 times, and the purity of the blue beads (rare target) in magnetic fraction was quantitatively measured with flow cytometry (method described separately).

To evaluate the performance of SMD during target release, both red and blue target beads were initially captured by MBs and then rare blue target beads were released via SMD. For each blue: red bead ratio, DNA-antibody conjugates against red (goat anti-human Ab/EP3) and blue (goat anti-mouse Ab/EP2) targets were added to the mixture at a final concentration of 2 µg/mL each, incubated for 15 minutes, and washed through centrifugation (at 3000 g for 2 minutes) 4 times. Meanwhile, complementary CPs (CP2 and CP3) were mixed at even proportion (1 µM each) with $2x10^7$ MBs, incubated for 15 minutes, and washed 4 times with a magnet. The fluorescent beads were then mixed with MB-CP at a constant ratio of 50 MBs per red fluorescent bead, incubated for 30 minutes, isolated with a magnet (thus enriching both red and blue targets), and washed 3 times. Following magnetic capture, DP2 (corresponding to release of blue beads) was added to the sample at 5 µM final concentration, mixed gently with pipette for 1 minute, and placed immediately on the magnet for collection of released beads in the supernatant. The sample was washed 3 times, and the supernatant fractions were pooled together. The purity of blue beads (rare target) in the supernatant fraction was quantitatively measured with flow cytometry (method described separately).

Three independent trials for each experiment were conducted to evaluate reproducibility. All conditions tested are summarized in Table 8.

Quantitative Analysis with Flow Cytometry

Flow cytometry on LSR-II (BD Biosciences) machine was used to count the number of fluorescent beads for calculations of purity and yield of isolated fractions. In order to compare relative bead counts, all samples were reconstituted in the same 100 µL volume, and a 96-well plate setup was used to consistently analyze an equal volume of each sample. A total of 5 channels were used for bead identification and enumeration. Forward scatter (FSC-A) was used to discriminate particles based on size, such that small particulates were not included in further analysis. Four different excitation lasers and 4 band-pass filters were used to uniquely identify a single bead color, as listed in Table 9. With this setup, beads were easily distinguished by their respective channel, and no compensation was necessary. For each specimen, at least 3000 beads were counted (lower counts for some cases in Figure S6, where low target concentration was used). Flow cytometry data was analyzed in FlowJo 9.3.3 (TreeStar). The total number of fluorescent beads was calculated by summing the counts from each of the four excitation/emission channels. Purities are reported as the number of beads of one color, divided by the total number of fluorescent beads within the sample. The overall yield is reported as the number of beads isolated into their respective fraction, divided by the number of beads of the same color counted within the reference sample that did not undergo magnetic sorting.

Qualitative Analysis with Fluorescence Imaging

IX-71 inverted fluorescence microscope (Olympus) equipped with true-color camera (QColor5, Olympus) and spectral imaging camera (Nuance, CRI, covering 420-720 nm spectral range) was used for imaging of fluorescent beads. Low-magnification images were obtained with 20x dry objective (NA 0.75, Olympus) and high-magnification with either 40x oil-immersion objective (NA 1.30, Olympus) or 100x oil-immersion objective (NA 1.40, Olympus). Wide UV filter cube (330-385 nm band-pass excitation, 420 nm long-pass emission, Olympus) was used for imaging of blue beads, FITC LP cube (460-500 nm band-pass excitation, 510 nm long-pass emission, Chroma) for green beads, Rhodamine LP cube (530-560 nm band-pass excitation, 572 nm long-pass emission, Chroma) for yellow beads, and Cy5 LP cube (590-650 nm band-pass excitation, 665 nm long-pass emission, Chroma) for red beads. All images were acquired for beads deposited on the surface of a glass cover slip. For 4-color bead imaging, images obtained with individual filter cubes were false-colored and merged into a composite image in Photoshop (Adobe Systems). Background was removed, and brightness and contrast were adjusted for best visual representation and clarity. Representative example of image processing is shown in Figure 2.

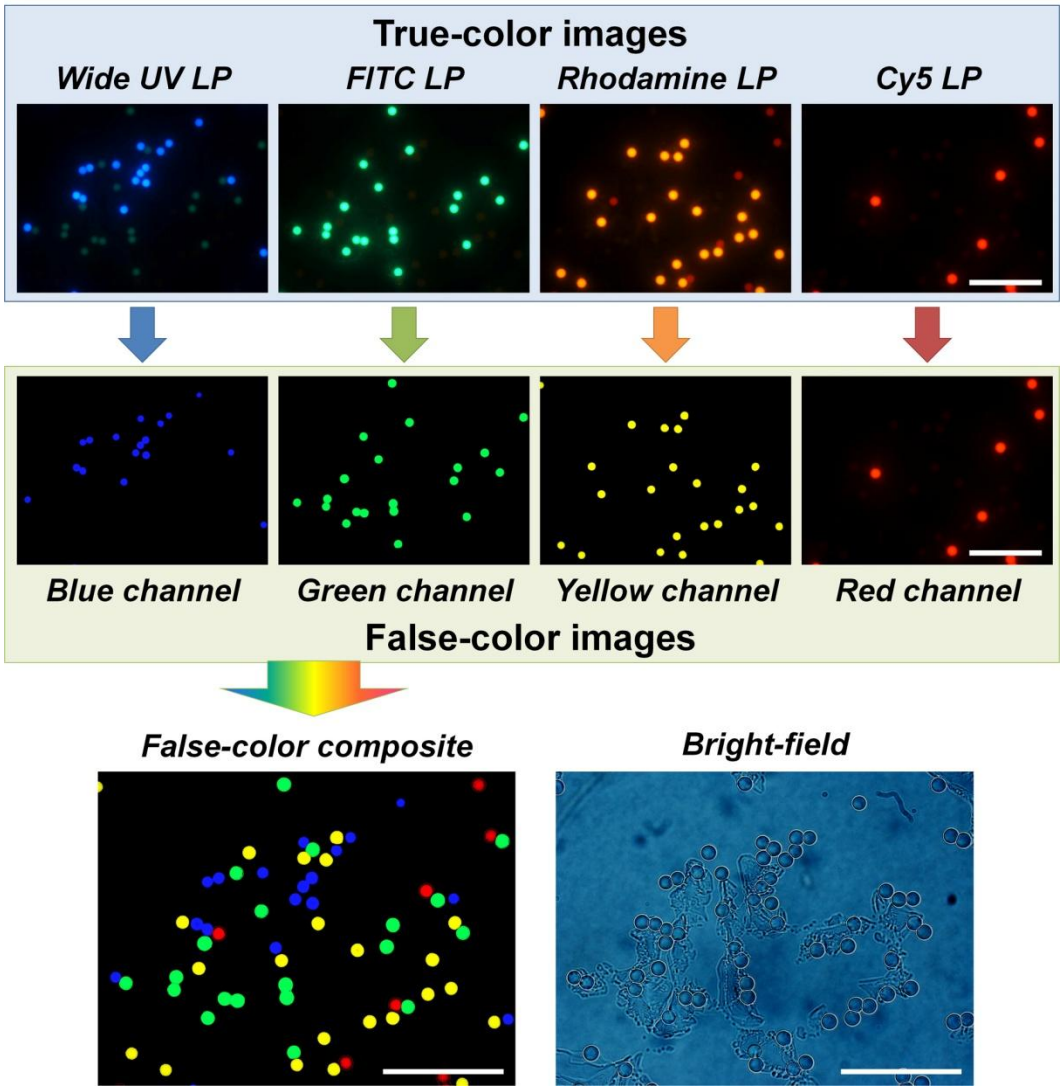

Figure 2. Schematic of fluorescence image processing. Each bead type is imaged with a filter cube best matching excitation/emission profile of a corresponding organic dye. With a set of 4 filter cubes indicated, individual true-color images contain mostly the signal from one fluorescent bead type, with minor spectral leak from adjacent colors. Application of a proper threshold eliminates such leaked signal along with the overall background, leaving only dominating signal from a single bead type. This signal is then false-colored for

better clarity of presentation. Merging of four false-color channels produces composite 4-color image, where each fluorescent bead is accounted for (compared to bright-field image) and represented by its corresponding color, thus enabling quick qualitative evaluation of the sample composition. Scale bar 50µm.

Table 1. DNA sequences used for multi-target enrichment and isolation. To demonstrate multi-target enrichment and isolation, 3 sets of DNA sequences **were** designed with 16 base-pair overlap (shown in red) between CP and EP and a 6 base-pair toehold region, allowing for a total of 22 base-pair DP binding. The toehold region is bolded. 10A spacer at the 5' end of EP and CP is in black.

Set	CP, EP, and DP sequences
CP1	5’ AAAAAAAAAA**TGTGAA**TAGACTTGCCATACGT 3'
EP1	5’ AAAAAAAAAAACGTATGGCAAGTCTA 3'
DP1	5’ ACGTATGGCAAGTCTA**TTCACA** 3'
CP2	5’ AAAAAAAAAA**TACCGT**AATTCTTGAGACCAGG 3'
EP2	5’ AAAAAAAAAACCTGGTCTCAAGAATT 3'
DP2	5’ CCTGGTCTCAAGAATT**ACGGTA** 3'
CP3	5’ AAAAAAAAAA**GCATTG**TTCCCTAGCGTCATCT 3'
EP3	5’ AAAAAAAAAAAGATGACGCTAGGGA 3'
DP3	5’ AGATGACGCTAGGGAA**CAATGC** 3'

Table 2. Conditions for the study of target capture kinetics

	Capture antibody type	MB type
Condition 1: Biotin-streptavidin mediated capture	Goat anti-Rabbit/Biotin	Streptavidin
Condition 2: Capture via complementary DNA hybridization	Goat anti-Rabbit/EP1	CP1
Condition 3: Non-complementary DNA hybridization	Goat anti-Rabbit/EP1	CP2
Condition 4: Mismatched antibody binding	Goat anti-Mouse/EP1	CP1
Condition 5: Nonspecific binding	None	Streptavidin

Table 3. Conditions for the study of target release kinetics

	DP
Condition 1: Release through complementary DP	DP1
Condition 2: Release through non-complementary DP	DP2
Condition 3: Release with no SMD	None

Table 4. Conditions for the study of antibody-antigen binding specificity for IgG-biotin

	Capture antibody type	MB type
Condition 1: Blue bead (Mouse IgG coating) capture	Goat anti-Mouse/Biotin	Streptavidin
Condition 2: Green bead (Rabbit IgG coating) capture	Goat anti-Rabbit/Biotin	Streptavidin
Condition 3: Red bead (Human IgG coating) capture	Goat anti-Human/Biotin	Streptavidin
Condition 4: Control (non-specific MB binding)	None	Streptavidin

Table 5. Conditions for the study of antibody-antigen binding specificity for IgG-DNA

	Capture antibody type	MB type
Condition 1: Blue bead (Mouse IgG coating) capture	Goat anti-Mouse/EP2	CP2
Condition 2: Green bead (Rabbit IgG coating) capture	Goat anti-Rabbit/EP1	CP1
Condition 3: Red bead (Human IgG coating) capture	Goat anti-Human/EP3	CP3
Condition 4: Control (non-specific MB binding)	None	Streptavidin

Table 6. Conditions for the study of EP-CP hybridization specificity for IgG-DNA

	Capture antibody type	MB type
Condition 1: Blue bead (Mouse IgG coating) capture	Goat anti-Rabbit/EP1 Goat anti-Mouse/EP2 Goat anti-Human/EP3	CP2
Condition 2: Green bead (Rabbit IgG coating) capture	Goat anti-Rabbit/EP1 Goat anti-Mouse/EP2 Goat anti-Human/EP3	CP1
Condition 3: Red bead (Human IgG coating) capture	Goat anti-Rabbit/EP1 Goat anti-Mouse/EP2 Goat anti-Human/EP3	CP3
Condition 4: Control (non-specific MB binding)	Goat anti-Rabbit/EP1 Goat anti-Mouse/EP2 Goat anti-	Streptavidin

	Human/EP3	

Table 7. Conditions for the study of SMD specificity

	Capture antibody type	MB type	DP
Condition 1: Blue bead (Mouse IgG coating) release	Goat anti-Rabbit/EP1 Goat anti-Mouse/EP2 Goat anti-Human/EP3	CP1/CP2/CP3	DP2
Condition 2: Green bead (Rabbit IgG coating) release	Goat anti-Rabbit/EP1 Goat anti-Mouse/EP2 Goat anti-Human/EP3	CP1/CP2/CP3	DP1
Condition 3: Red bead (Human IgG coating) release	Goat anti-Rabbit/EP1 Goat anti-Mouse/EP2 Goat anti-Human/EP3	CP1/CP2/CP3	DP3
Condition 4: Control (non-specific target release)	Goat anti-Rabbit/EP1 Goat anti-Mouse/EP2 Goat anti-Human/EP3	CP1/CP2/CP3	None

Table 8. Conditions for the study of SMD selectivity at varying target abundance

	Capture antibody type	MB type	DP
Condition 1: Blue bead (Mouse IgG coating) capture via biotin-streptavidin	Goat anti-Mouse/Biotin	Streptavidin	N/A
Condition 2: Blue bead (Mouse IgG coating) capture via DNA-antibody conjugate	Goat anti-Mouse/EP2	CP2	N/A
Condition 3: Blue bead (Mouse IgG coating) release via SMD	Goat anti-Mouse/EP2 Goat anti-Human/EP3	CP2/CP3	DP2

Table 9. Flow-cytometry parameters used for bead counting

Microsphere	Laser	Emission filter
Blue	350 nm	450/40 nm
Green	488 nm	530/30 nm
Yellow	561 nm	610/20 nm
Red	641 nm	710/50 nm

Results and Discussion

Antigen-coated fluorescent microspheres: a model system for cell sorting

Although SMD-based magnetic sorting represents a platform technology applicable to a wide range of analytes, proof-of-concept work reported here most closely resembles conditions necessary for sorting of live cells, a significant application of this technology. In this setup, four-color fluorescent beads of size similar to mammalian cells are used as a model system for development and characterization of SMD technology. Fluorescent beads are easy to identify and count, and are thus ideal for technology characterization and validation. To magnetically isolate specific cell populations, antibodies against cell-specific surface markers are used. Thus, using fluorescent beads as a model system for cell sorting first requires surface modification with an identifying antigen. In these experiments, mouse, rabbit, and human IgGs were selected as the identifying antigens for blue, green, and red beads respectively; yellow beads were left unmodified to serve as an impurity population to remove. To attach antigen to the surface of carboxylated fluorescent beads, a two-step carbodiimide covalent conjugation protocol was developed (see Methods). To validate the conjugation procedure, the presence and density of a specific antigen on the surface of fluorescent beads, 2-step staining using biotinylated secondary antibodies for antigen detection and red-emitting quantum dots for fluorescent labeling was applied (Figure 3). Red quantum dots (emitting at 655 nm) exhibit very large Stokes shift and high brightness, enabling easy unmixing of Qdot signal from the fluorescence of target beads and quantitative analysis of staining intensity, while using single UV source for excitation of all samples. Positive staining appears as red ring around target beads on false-color images (merged Qdot and fluorescent bead channels) and as high-intensity signal on black-and-white inserts (Qdot

channel only). All insert images (Qdot channel) were normalized by imaging parameters, thus enabling direct comparison of staining intensity between different bead types. Blue, green, and red beads develop bright positive staining only for antigens that were conjugated to their surface (i.e. blue for mouse IgG, green for rabbit IgG, and red for human IgG), while showing no cross-reactivity with other antibodies or Qdots alone (control). Unconjugated yellow beads, which were used as an "impurity" population throughout all studies, failed to produce staining with any antibody, as expected.

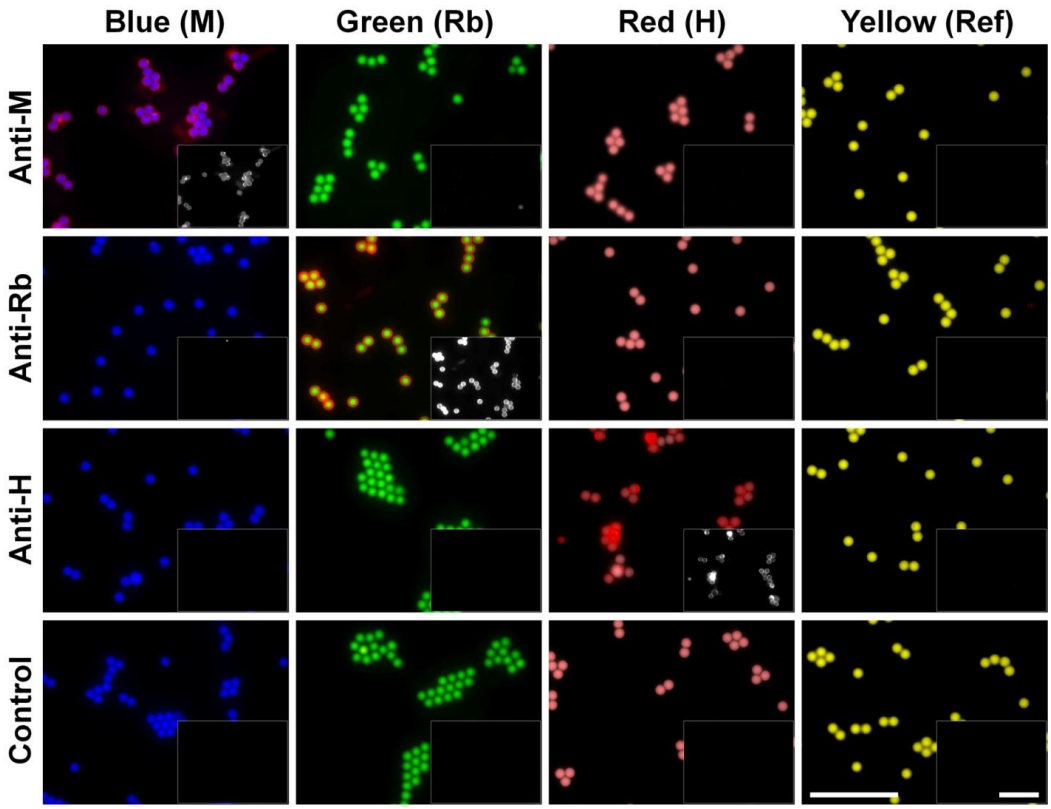

Figure 3. Validation of antigen coating on the surface of fluorescent beads. Specific staining is only detected along the diagonal axis (see inset) where secondary IgG binds its cognate antigen. Scale bar 50µm.

Kinetics and specificity of target capture and release

For any biomolecule separation method, both the overall performance and duration of the separation method are critical considerations. While maximizing the specificity of the method improves purity and yield, minimizing the duration of the separation procedure reduces the effort required for the procedure and helps preserve the biological characteristics of the target. Here, kinetics and specificity of the magnetic capture and SMD-based release were first evaluated using single-color green microspheres (see Methods, Table 2). As shown in Figure 4a, target capture through hybridization between EPs and CPs slightly lags behind that mediated by the gold standard streptavidin-biotin interaction, but both reach nearly complete target capture at a 1 hour time point (>98%). Representative fluorescence micrographs taken for the unbound (supernatant) and MB-bound fractions for matched and mismatched DNA sequences after a 60-min incubation period are shown in Figure 4 b-e. Clearly, the matched EP1/CP1 pairs lead to nearly complete capture of target beads in the MB-bound fraction, whereas the mismatched sequences (CP2) produce only negligible non-specific binding.

Following magnetic capture via DNA linkers, the specificity and kinetics of target release via SMD were evaluated (see Methods, Table 3). Target release was measured after 1 min or 60 min incubation periods (Figure 5a). Remarkably, even after 1 min of SMD, release of target beads into the supernatant is nearly complete (97 %) for complementary DP, while only minimal nonspecific release (< 3 %) is observed for the mismatched DP and reference, demonstrating high selectivity and speed of SMD despite potential issues such as steric hindrance. Fluorescence microscopy (Figure 5b-e) further corroborates this conclusion. The outstanding kinetics and selectivity of SMD is enabled by three fundamental features of this technology. First, as mentioned earlier, DNA displacement with longer complementary strands is an extremely selective and fast process. Second, diffusion of small DNA strands to microbeads is much faster than diffusion

between two microparticles, meaning the kinetics of target release can be much faster than target capture. Third, a profound impact originates from the differential concentrations in the separation reaction. In the case of conventional immunomagnetic separation, the two 'reactants' are MBs and targets, which are often used in fM to pM concentration range [18, 24]. In SMD, on the other hand, the two 'reactants' are MB-target complexes and single-stranded DNA with concentration typically in the µM range, which is six to nine orders of magnitude higher than that of MBs, thus driving the reaction rate. Noteworthy, there is virtually no non-specific target release for 1 min and 60 min incubation periods, indicating that the 16 base pair EP-CP overlap offers sufficient long-term stability (under gentle rotating agitation). Yet, vigorous washing results in more noticeable non-specific target release with DNA links compared to biotin-streptavidin bond (data not shown). Such behavior is not surprising, as DNA-DNA binding strength (20-50 pN for 10-30 base pairs) [25] is considerably lower than that of biotin-streptavidin bond (300 pN) [26]. Poor bond stability can be partially addressed by using longer DNA probes, while maintaining binding specificity through careful sequence design. Furthermore, this effect may be negligible for separation of smaller analytes (proteins, bacteria), as shear forces decrease along with particle size.

The specificity of SMD technology was characterized in greater depth using four-color bead mixes, as the overall performance of the technology requires high specificity for each primary-secondary antibody pair and each set of DNA sequences. Figure 6 shows the specificity of target (blue, red, or green) capture from a 4-bead mix for standard magnetic isolation (via streptavidin-biotin bond formation, see Methods, Table 4). The purity of magnetic fraction captured was calculated using flow cytometry as a measure of binding selectivity. For the standard capture method, specificity of antibody-antigen recognition was tested (Figure 6A), while for SMD technology, both specificity of antibody-antigen recognition by DNA-antibody conjugates (Figure 6B) and specificity of DNA

hybridization between encoding and capture probes (Figure 6C) were evaluated. As evident from Figure 6C, very high selectivity of target capture via EP-CP hybridization is obtained (with purities ranging from 96.9% to 98.9%). At the same time, antibodies exhibit some cross-reactivity, producing red bead impurity in green bead captured fraction (due to binding of anti-rabbit antibody to human IgG on red beads) and blue bead impurity in red bead captured fraction (due to binding of anti-human antibody to mouse IgG on blue beads) above background values in both streptavidin-biotin bond-mediated capture (Figure 6A) and SMD-based capture (Figure 6B). In the control, only minor non-specific binding is observed between MBs and "target" (blue, green, and red) as well as "impurity" (yellow) beads.

In a similar manner, specificity of SMD-based release of each target bead (blue, green, or red) from a MB-captured 3-bead mix was also tested to demonstrate the selectivity of each displacement probe sequence (Figure 7). The purity of isolated (unbound) fraction was calculated using flow cytometry as a measure of DNA displacement selectivity. Both qualitative evaluation with fluorescence microscopy (Figure 7A) and quantitative analysis of flow cytometry data (Figure 7B) indicate good selectivity of SMD, as evidenced by the moderate purities of isolated target fractions above ~92%. Trace amounts of yellow beads are present in all fractions due to initial non-specific capture from a 4-bead mix. Some non-specific release of red and blue targets observed here might, in part, be explained by the lower antigen coating on these beads compared to green beads, as indicated by lower Qdot staining intensity in Figure 3. Effect of differential antigen surface coverage can be negated to some extent by adjusting the number of corresponding capture probes on MBs (i.e. increasing CP coverage on MB should improve binding with targets exhibiting lower density of surface antigen). Following this logic, SMD-based 4-bead sorting study presented in Figure 8 (see next section) was performed using a 2:2:1 ratio of CPs on MBs for red, blue, and green targets respectively, which increased purity to ~95% for each target. To further confirm

that non-specific target release results from the rupture of DNA link due to mechanical forces rather than due to SMD by non-complementary DPs, we compared the fraction of beads released in cases with and without DP added (Figure 7C). As evident from the quantitative analysis of flow cytometry data, non-specific target release does not depend on the presence of DPs, showing no statistically significant difference between levels of impurities in all cases ($p>0.05$ based on two-tailed t-test), except for the blue bead impurity in the green bead fraction, which is actually lower than in control case.

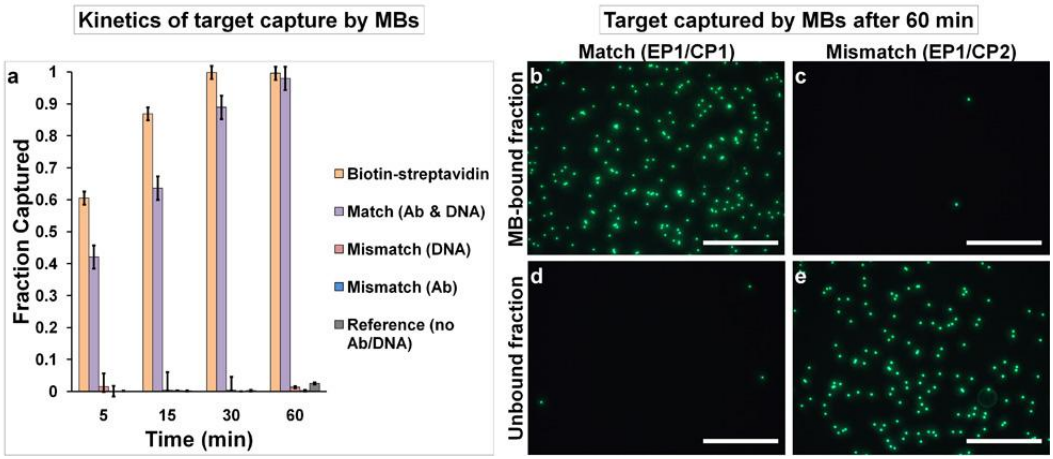

Figure 4. Kinetics and specificity of target capture in single-target experiment. (a) Quantitative analysis of target capture through DNA hybridization. Average of 3 separate experiments is shown. Error bars indicate one standard deviation. (b-e) Qualitative evaluation of target capture with fluorescence microscopy. Targets (green) are retained in MB-bound fraction for complementary EP1/CP1 link (b,d), but not for non-complementary EP1/CP2 link (c,e). Scale bar 250 μm.

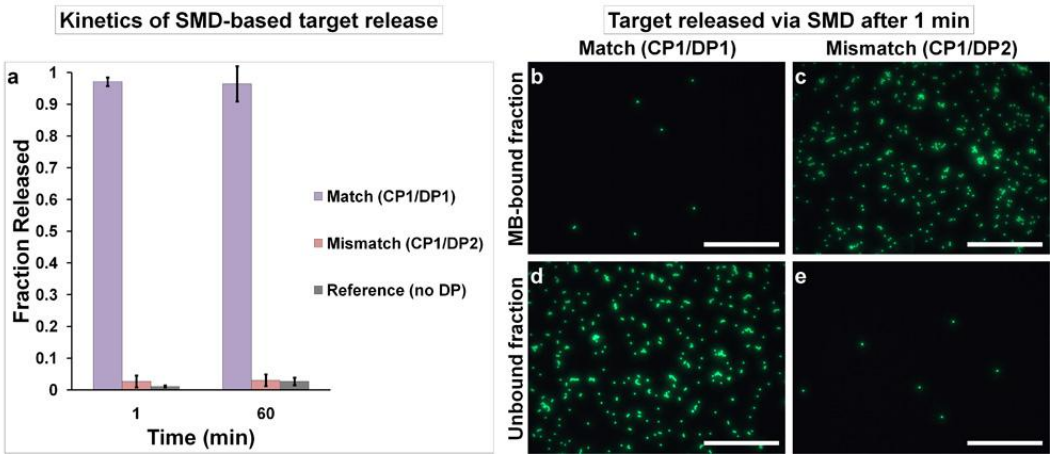

Figure 5. Kinetics and specificity of target release in single-target experiment. Kinetics and specificity of target release. (a) Quantitative analysis of SMD-based target release kinetics. Average of 3 separate experiments is shown. Error bars indicate one standard deviation. (b-e) Fluorescence microscopy evaluation of target release yield and specificity. Nearly complete release of targets (green beads) into supernatant is obtained with complementary (b,d)but not non-complementary (c,e) DPs. Scale bar 250 μm.

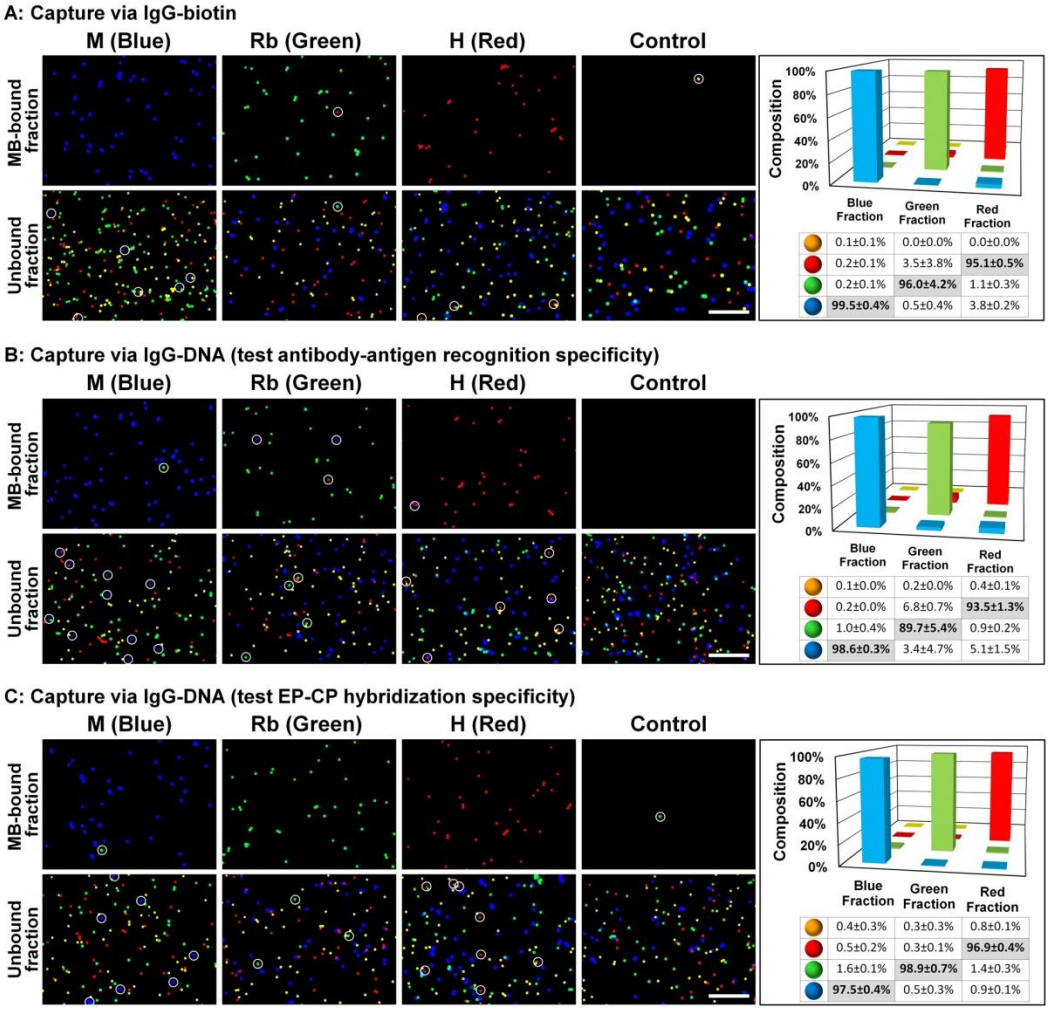

Figure 6. Specificity of target capture in multi-target experiment. Specificity of capture of each "target" bead (blue, green, or red) from a 4-bead mix was tested for standard magnetic isolation (via streptavidin-biotin bond formation) as well as for SMD technology. Representative fluorescence images are shown for each study, and impurities are highlighted with white circles. Quantitative analysis of purities of isolated fractions is presented in respective histograms and tables (right panels), and the average value and standard deviation of 3 independent experiments is reported. Scale bar 100μm.

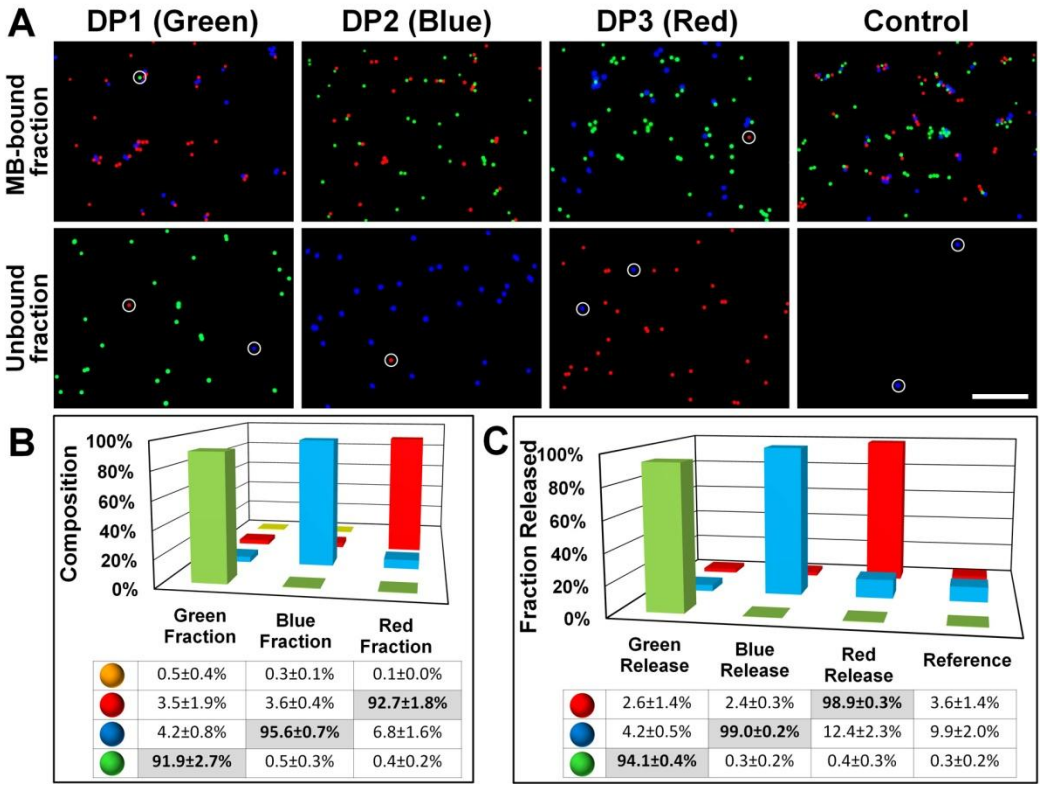

Figure 7. Specificity of target release in multi-target experiment. Specificity of SMD-based release of each "target" bead (blue, green, or red) from a MB-captured 3-bead mix was tested. Average value and standard deviation of 3 independent experiments is reported in quantitative analysis (Figure 7B and Figure 7C). Impurities are indicated by white circles on fluorescence images (Figure 7A).Scale bar 100µm.

Characterization of SMD Technology Performance

The overall goal of this project is to transform conventional magnetic sorting into a multiplexed format while preserving the traditional benefits of magnetic separation, including high throughput, simple instrumentation, ease of use, and speed. Previous sections have demonstrated the potential for SMD technology to achieve this goal by demonstrating its high selectivity and rapid separation kinetics using fluorescent microspheres as a model system. Within this section, we further characterize SMD performance in some magnetic separation scenarios, including (1) separation of a four-bead mixture into purified fractions using SMD technology, (2) a comparison with separation of a four-bead mixture using conventional sequential magnetic separation, and (3) the effects of varying target abundance on both separation procedures.

First, the utility of SMD technology for quick sorting of multiple targets from a mixed sample was demonstrated (see Methods). In brief, four populations of fluorescent beads were first pooled in a single sample at even proportions. Beads of the three primary colors were tagged with distinct antigens on the surface (green with rabbit IgG, blue with mouse IgG, and red with human IgG), while unmodified yellow beads serve as an impurity for removal. Three antibodies specifically recognizing those surface antigens are tagged with unique encoding oligonucleotides (EP1, EP2, and EP3) and incubated with the mixture sample. In parallel, MBs are modified with CP1, CP2, and CP3, complementary to each EP. Following the procedure schematically illustrated in Figure 1b, the red, blue and green beads are simultaneously enriched magnetically and subsequently isolated one at a time by addition of their cognate DPs. Qualitative evaluation with fluorescence microscopy (Figure 4a-h) and quantitative analysis with flow cytometry (Figure 4i) reveal excellent purity (Red: 95.5%; Blue: 94.7%, and Green: 96.7%) and reproducibility (standard deviation < 1%) for each of the isolated fractions. The overall yield for each target (Red: 68.2±13.8%, Blue:

74.5±8.5%, and Green: 61.4±8.2%) was calculated by dividing the number of beads collected by that in the reference sample, which did not undergo the magnetic separation procedure. The sources of the loss may include dead volume in pipette tips, retention of beads on centrifuge tube walls/caps, incomplete magnetic capture, nonspecific release, and incomplete release of targets. These parameters deserve future optimization especially for separation and characterization of rare targets, such as stem cells or circulating tumor cells. Nevertheless, the yield and throughput reported herein marks a considerable improvement over previous multi-target magnetic selection methods, while requiring no sophisticated instrumentation.

To further highlight the benefits of SMD technology, we contrasted our approach to conventional sequential immunomagnetic sorting (Figure 9). Here, using biotinylated antibodies and streptavidin-coated MBs, we again isolated 3 targets from an initial mixture of 4 bead populations (see Methods). From a 4-bead mixture (consisting of 3 "target" fluorescent beads and yellow "impurity" at equal proportions) targets were isolated in the following order: red beads -> blue beads -> green beads, leaving "impurity" yellow beads in unbound fraction. Both qualitative evaluation with fluorescence microscopy (left panels) and quantitative analysis of flow cytometry data (histogram and table on the right) indicate high purity of the first isolated target (red, >98%) and markedly decreasing purity of subsequent isolation cycles (~92% purity for blue and ~90% for green beads), resulting mainly from contamination by the preceding target. Thus, not only is this process time consuming in comparison to SMD (requiring over 1.5 hours for each target isolated, for a total of ~5 hours), but also incomplete magnetic capture of any given target creates impurities for targets isolated in downstream steps. We attributed this effect to incomplete magnetic capture of a given target, where biotinylated antibody remained on the target surface, creating a biotin-labeled impurity for capture via streptavidin during the next isolation cycle. Although this issue can potentially be circumvented by using unique secondary-affinity ligands,

availability of such ligands is limited, falling far behind the multiplexing potential offered by DNA. At the same time, potential incomplete target release with SMD does not result in additional impurities in downstream fractions, as unique DPs are used for release of each target. Also, it is worth noting that yields achieved with sequential sorting (red: 73.8 ± 16.1% , blue: 70.4 ± 16.3%, green: 53.8 ± 7.7%) are comparable to SMD approach (red: 68.2 ± 13.8%, blue: 74.5 ± 8.5%, green: 61.4 ± 8.2%), with losses mainly attributed to bead loss during sample handling (washing/pipetting).

Finally, we tested the dynamic range for multi-target SMD separation by systematically decreasing the ratio of target to impurity florescent beads, as large variations in target concentration can be expected with certain practical applications (Figure 10). Expectedly, purity of target captured from a mix of beads in solution (Figure 10A) as well as purity of target released from a MB-bound fraction containing multiple bead types (Figure 10B) suffers from decreasing test target abundance (and increasing proportion of reference beads). With this, target capture demonstrates higher selectivity compared to target release (e.g. purity of capture via DNA hybridization drops from 98.4 ± 1.0% to 43.0 ± 4.0% with target abundance decreasing from 50% to ~1%, whereas purity of release via SMD drops from 94.8 ± 1.0% to 20.0 ± 9.9%). However, it should be noted that an issue of isolation of rare targets at high purity is not unique to SMD technology, as similar drop in target purity at decreasing target abundance is observed with more conventional magnetic isolation via streptavidin-biotin bond formation (showing a drop of captured target purity from 99.5 ± 0.2% at equal bead proportion to 62.1 ± 7.5% at 1:100 test-to-reference bead ratio). Also, it is worth mentioning that the increase in error bar magnitude observed with decreasing test target abundance mainly results from a shot noise introduced by the low absolute number of test beads within the sample, with actual test bead counts from flow cytometry dropping from ~3000 to only ~30 when target abundance is decreased from 1:1 to 1:100. Inferring from the control studies

(Figure 4 and 5) and similar performance of biotin-streptavidin mediated capture (Figure 9), we believe that major causes for this effect are antibody cross-reactivity, incomplete washing, and rupture of DNA links. Therefore, further protocol optimization is required for applications where targets are present at high dynamic range.

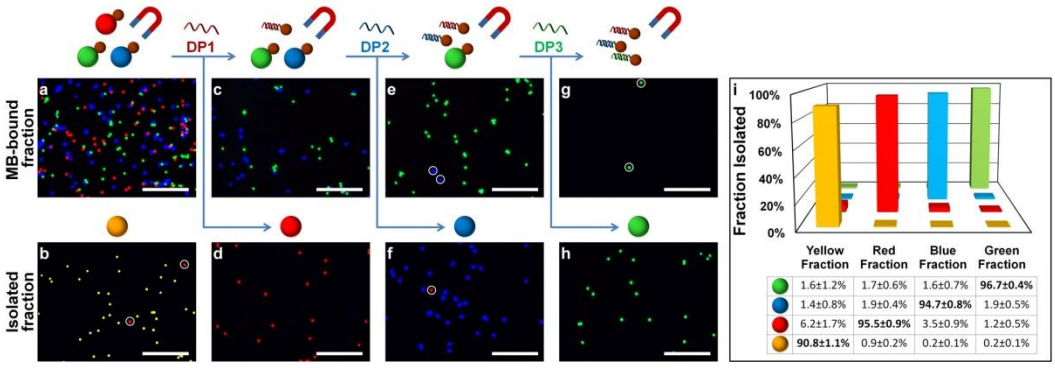

Figure 8. Rapid multi-target SMD-based sorting. (a-h) Fluorescence microscopy of MB-bound (a-d) and isolated (e-h) fluorescent bead fractions at different stages of SMD-based sorting. Immunomagnetic isolation of 3 targets (red, green, and blue beads) retains targets within MB-bound fraction (a), leaving "impurity" (yellow beads) in supernatant (e). Sequential introduction of target-specific DPs leads to selective release of a target into supernatant (f,g,h), leaving non-displaced targets in MB-bound fraction (b,c,d). Impurities are indicated by white circles. Images are processed according to procedure outlined in Figure S4. Scale bar 100 µm (i) Quantitative analysis of purity of isolated fractions with flow-cytometry. Average and standard deviation from 3 separate experiments are shown.

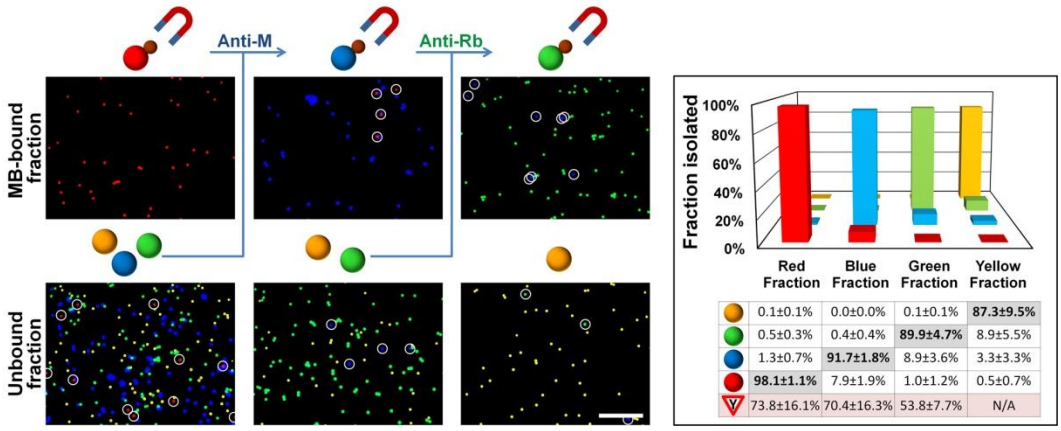

Figure 9. Multi-target sorting using sequential streptavidin-biotin bond-mediated target capture. 4-color bead sorting was done using antigen recognition by biotinylated antibodies followed by magnetic isolation of individual targets via streptavidin-biotin bond formation with streptavidin-coated MBs. Average value and standard deviation of 3 independent experiments is reported in quantitative analysis. Impurities are indicated by white circles on fluorescence images. Note: yellow yield is not applicable (N/A) because no magnetic capture step was performed. Scale bar 100µm.

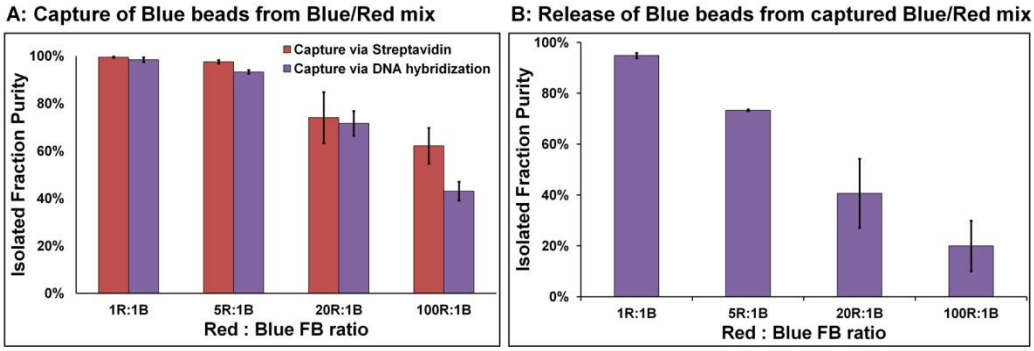

Figure 10. SMD-based sorting selectivity at varying target abundance. Samples were prepared with test-to-reference bead ratio of 1:1, 1:5, 1:20, and 1:100 (holding concentration of reference and MBs constant). Purity of isolated test target fraction was determined by flow cytometry, with an average value and standard deviation of 3 independent experiments reported.

Conclusions and future directions

In summary, the work described within this document demonstrates a simple yet robust multi-target immunomagnetic separation technology based on the clever concept of DNA strand-mediated displacement. Magnetic separation serves as a high-throughput platform for sorting of a wide array of targets, while DNA-antibody conjugates enable highly multiplexed indirect selection, which confers important benefits of high target yield and purity. Finally, rapid target sorting is enabled by SMD technology via fast DNA binding and displacement, fast diffusion of relatively small DPs, and high concentration of DNA reactants. Overall, combination of these critical components provides a unique solution to a long-standing problem in magnetic separation: multi-target sorting at high yield, purity, and throughput.

This work provides strong evidence that the versatility of SMD-based separation platform will enable a number of powerful applications, such as live cell sorting, as both target capture through DNA hybridization and SMD can be carried out in a range of cell- and bio-compatible buffers and at ambient or chilled conditions. Further, SMD technology might streamline implementation of conventional immunomagnetic selection where MBs must be removed to avoid interference with further analysis or adverse effects on target biological state [27-29], as well as to allow further isolation via a different surface epitope of the same target, thus enabling multi-parameter selection. Finally, availability of DNA-antibody conjugates on target surface following MB release should enable isolation of rare targets by applying several selective rounds of magnetic capture and SMD release.

As previously mentioned, SMD technology can be applied to the separation of virtually any bioanalyate (i.e. cells, proteins, DNA), and thus applications for SMD technology extend beyond the cell-sorting application explored in-depth

within this document. For example, this researcher has also explored the use of SMD for protein detection using enzyme-linked immunosorbent assay (ELISA), and has acquired promising preliminary data both on a traditional 96-well plate format as well as a MB-based ELISA (data not included). Commercialized multiplexed ELISAs have been developed, mainly the Mosaic (R&D systems) approach that involves spotting multiple capture antibodies to a single plate-well, a form of spatial multiplexing. However, it is generally required that pre-spotted plates are obtained through a commercial vendor, thus prohibiting the development of customized assays designed for specific research applications. Using SMD, it is possible to modify a traditional ELISA to capture and detect multiple antigens of interest by tagging each detection antibody with a specific DNA sequence. Incubation steps with complementary DNA-biotin, followed by binding with horseradish peroxidase (HRP)-streptavidin can be applied to complete the assay, making it possible to detect multiple antigens bound to a single well or MB sample through displacement and development of the DNA-biotin: streptavidin-HRP complex and color formation with a development buffer. In this setup, multiplexing is achieved via DNA-linkage rather than spatial multiplexing, thus circumventing the need to pre-spot plates.

Copyright Note

Many figures and texts within this Master's thesis have been taken with permission from an earlier publication of this work in the Journal of the American Chemical society by this author [30].

References

1. Almand, B., et al., *Clinical Significance of Defective Dendritic Cell Differentiation in Cancer.* Clinical Cancer Research, 2000. **6**(5): p. 1755-1766.
2. Mackensen, A., et al., *Phase I Study of Adoptive T-Cell Therapy Using Antigen-Specific CD8+ T Cells for the Treatment of Patients With Metastatic Melanoma.* Journal of Clinical Oncology, 2006. **24**(31): p. 5060-5069.
3. Olsvik, O., et al., *Magnetic separation techniques in diagnostic microbiology.* Clin. Microbiol. Rev., 1994. **7**(1): p. 43-54.
4. Stamm, C., et al., *Autologous bone-marrow stem-cell transplantation for myocardial regeneration.* The Lancet, 2003. **361**(9351): p. 45-46.
5. Bailey, R.C., et al., *DNA-Encoded Antibody Libraries: A Unified Platform for Multiplexed Cell Sorting and Detection of Genes and Proteins.* Journal of the American Chemical Society, 2007. **129**(7): p. 1959-1967.
6. Bonner, W.A., et al., *Fluorescence Activated Cell Sorting.* Review of Scientific Instruments, 1972. **43**(3): p. 404-409.
7. Fu, A.Y., et al., *A microfabricated fluorescence-activated cell sorter.* Nature Biotechnology, 1999. **17**(11): p. 1109-1111.
8. Miltenyi, S., et al., *High gradient magnetic cell separation with MACS.* Cytometry, 1990. **11**(2): p. 231-238.
9. Šafařík, I. and M. Šafaříková, *Use of magnetic techniques for the isolation of cells.* Journal of Chromatography B: Biomedical Sciences and Applications, 1999. **722**(1-2): p. 33-53.
10. Pruszak, J., et al., *Markers and methods for cell sorting of human embryonic stem cell-derived neural cell populations.* Stem Cells, 2007. **25**(9): p. 2257-68.
11. Chalmers, J.J., et al., *Flow Through, Immunomagnetic Cell Separation.* Biotechnology Progress, 1998. **14**(1): p. 141-148.
12. Inglis, D.W., et al., *Continuous microfluidic immunomagnetic cell separation.* Applied Physics Letters, 2004. **85**(21): p. 5093-5095.
13. Liu, C., et al., *On-chip separation of magnetic particles with different magnetophoretic mobilities.* Journal of Applied Physics, 2007. **101**(2): p. 024913.
14. Yavuz, C., et al., *Low-Field Magnetic Separation of Monodisperse Fe3O4 Nanocrystals.* Science, 2006. **314**(5801): p. 964-967.
15. Yellen, B.B., et al., *Traveling wave magnetophoresis for high resolution chip based separations.* Lab on a Chip, 2007. **7**(12): p. 1681-1688.
16. Adams, J.D., U. Kim, and H.T. Soh, *Multitarget magnetic activated cell sorter.* Proceedings of the National Academy of Sciences of the United States of America, 2008. **105**(47): p. 18165-18170.

17. Semple, J.W., et al., *Rapid separation of CD4+ and CD19+ lymphocyte populations from human peripheral blood by a magnetic activated cell sorter (MACS).* Cytometry, 1993. **14**(8): p. 955-60.
18. Tiwari, A., et al., *Magnetic beads (Dynabead™) toxicity to endothelial cells at high bead concentration: Implication for tissue engineering of vascular prosthesis.* Cell Biology and Toxicology, 2003. **19**(5): p. 265-272.
19. Bath, J. and A.J. Turberfield, *DNA nanomachines.* Nature Nanotechnology, 2007. **2**(5): p. 275-284.
20. Chen, Y. and C. Mao, *Putting a Brake on an Autonomous DNA Nanomotor.* Journal of the American Chemical Society, 2004. **126**(28): p. 8626-8627.
21. Shin, J.-S. and N.A. Pierce, *A Synthetic DNA Walker for Molecular Transport.* Journal of the American Chemical Society, 2004. **126**(35): p. 10834-10835.
22. Zhang, D.Y. and G. Seelig, *Dynamic DNA nanotechnology using strand-displacement reactions.* Nat Chem, 2011. **3**(2): p. 103-13.
23. Yurke, B. and A. Mills, *Using DNA to Power Nanostructures.* Genetic Programming and Evolvable Machines, 2003. **4**(2): p. 111-122.
24. Pilling, D., et al., *The kinetics of interaction between lymphocytes and magnetic polymer particles.* Journal of Immunological Methods, 1989. **122**(2): p. 235-41.
25. Strunz, T., et al., *Dynamic force spectroscopy of single DNA molecules.* Proceedings of the National Academy of Sciences of the United States of America, 1999. **96**(20): p. 11277-11282.
26. Zlatanova, J., S.M. Lindsay, and S.H. Leuba, *Single molecule force spectroscopy in biology using the atomic force microscope.* Progress in Biophysics and Molecular Biology, 2000. **74**(1-2): p. 37-61.
27. Nie, C.Q., et al., *CD4+ CD25+ Regulatory T Cells Suppress CD4+ T-Cell Function and Inhibit the Development of Plasmodium berghei-Specific TH1 Responses Involved in Cerebral Malaria Pathogenesis.* Infection and Immunity, 2007. **75**(5): p. 2275-2282.
28. Roberts, S.J., et al., *Characterizing tumor-promoting T cells in chemically induced cutaneous carcinogenesis.* Proceedings of the National Academy of Sciences of the United States of America, 2007. **104**(16): p. 6770-6775.
29. Russell, M.S., et al., *A Reduced Antigen Load In Vivo, Rather Than Weak Inflammation, Causes a Substantial Delay in CD8+ T Cell Priming against Mycobacterium bovis (Bacillus Calmette-Guérin).* Journal of Immunology, 2007. **179**(1): p. 211-220.
30. Probst, C.E., P. Zrazhevskiy, and X. Gao, *Rapid Multitarget Immunomagnetic Separation through Programmable DNA Linker Displacement.* Journal of the American Chemical Society. **133**(43): p. 17126-17129.